Thermodynamic characterization of yeast triosephosphate isomerase refolding: insights into the interplay between function and stability as reasons for the oligomeric nature of the enzyme

Hugo NÁJERA, Miguel COSTAS[1] and D. Alejandro FERNÁNDEZ-VELASCO[2]

Laboratorio de Fisicoquímica e Ingeniería de Proteínas, Departamento de Bioquímica, Facultad de Medicina, Universidad Nacional Autónoma de México, Ciudad Universitaria. México, D.F. 04510, México

The reasons underlying the oligomeric nature of some proteins such as triosephosphate isomerase (TIM) are unclear. It has been proposed that this enzyme is an oligomer, mainly because of its stability rather than for functional reasons. To address this issue, the reversible denaturation and renaturation of the homodimeric TIM from baker's yeast (*Saccharomyces cerevisiae*) induced by guanidinium chloride and urea have been characterized by spectroscopic, functional and hydrodynamic techniques. The unfolding and refolding of this enzyme are not coincident after 'conventional' equilibrium times. Unfolding experiments did not reach equilibrium, owing to a very slow dissociation and/or unfolding process. By contrast, equilibrium was reached in the refolding direction. The simplest equilibrium pathway compatible with the obtained data was found to be a three-state process involving an inactive and expanded monomer. The Gibbs energy changes for monomer folding ($\Delta G^0_{fold} = -16.6 \pm 0.7$ kJ · mol^{-1}) and monomer association ($\Delta G^0_{assoc} = -70.3 \pm 1.1$ kJ · mol^{-1}) were calculated from data obtained in the two denaturants. From an analysis of the present data and data from the literature on the stability of TIM from different species and for other β/α barrels, and model simulations on the effect of stability in the catalytic activity of the enzyme, it is concluded that the low stability of the monomers is neither the only, nor the main, cause for the dimeric nature of TIM. There is interplay between function and stability.

Key words: dimer evolution, equilibrium, hysteresis, monomeric intermediate, TIM-barrel, unfolding/refolding.

INTRODUCTION

The functional and regulatory properties of oligomeric proteins are mostly provided by quaternary structure formation [1,2]. Triosephosphate isomerase (TIM) is the prototype of the β/α barrel, one of the most common folds found in Nature [3,4]. All wild-type TIMs so far studied are oligomers. TIM activity exhibits classical Michaelis–Menten kinetics, is not allosterically regulated and the residues involved in substrate binding and catalysis are all located in the same subunit. However, dimerization is required for catalytic activity. In an effort to rationalize the oligomeric nature of TIM, it has been proposed that TIM monomers are thermodynamically unstable and that subunit assembly induces maximal conformational stability [5]. Besides this structural-stability explanation, it has been also argued that dimerization is necessary to optimize the geometry of the active-site pocket [6]. It appears that the relative importance of stability and function as reasons for the oligomeric nature of this enzyme is not convincingly established.

Some oligomers show a two-state dissociation/unfolding process without detectable intermediates [7]. However, in many cases, stable intermediates have been reported [8,9]. Where three or more states are observed, it is possible to estimate the relative contribution of monomer folding and association to the overall stability of the protein through the calculation of the thermodynamic parameters describing the processes involved. The two prerequisites for these calculations are the reversibility of the process and that the system reaches equilibrium. The equilibrium constants that describe the effect of denaturant concentration on the relative amounts of native, folding intermediates and unfolded states can be obtained from two types of experiment, namely (a) native dimer → unfolded monomer (N → U) unfolding experiments, where the native protein is the initial state and samples are incubated at several concentrations of denaturant, and (b) U → N refolding experiments in which the native protein is first completely unfolded using high denaturant concentrations. The unfolded state is therefore the initial state that is then allowed to refold at lower denaturant concentrations. In both types of experiments, the relative populations of the stable states are then measured after equilibrium is reached, monitoring the spectroscopic, functional or hydrodynamic properties of the system. If denaturation and renaturation are reversible and the incubation time is long enough for equilibrium to be reached, both types of experiment should give the same results. For oligomeric proteins, unfolding rather than refolding has been commonly studied, since low refolding yields are commonly observed owing to the formation of irreversible non-productive interactions between folding intermediates [9]. Another difficulty is that unfolding and refolding kinetics might be very slow, making the identification of the equilibrium states problematic. In fact, kinetic control has been observed in monomeric [10] and oligomeric proteins [11–15]. In the case of TIM, kinetic hysteresis between N → U and U → N experiments has been detected in the pressure-induced denaturation of rabbit TIM (rTIM) [16] and in the temperature-induced unfolding of baker's-yeast (*Saccharomyces cerevisiae*) TIM (yTIM) [17]. However, up until the present time, TIM stability has only been studied at equilibrium employing N → U experiments [5,18–24]. In the present study

Abbreviations used: DTT, dithiothreitol; GdmCl, guanidinium chloride; GDPH, glycerol-3-phosphate dehydrogenase; N → U, native dimer → unfolded monomer; R_s, Stokes radius; SCM, spectral centre of mass; TIM, triosephosphate isomerase; hTIM, human TIM; rTIM, rabbit TIM; TbTIM, *Trypanosoma brucei* TIM; yTIM, yeast (*Saccharomyces cerevisiae*) TIM.

[1] On sabbatical leave from the Departamento de Fisicoquímica, Facultad de Química, Universidad Nacional Autónoma de México, Ciudad Universitaria. México, D.F. 04510, México.

[2] To whom correspondence should be addressed (e-mail fdaniel@servidor.unam.mx).

we monitored the denaturation and renaturation of yTIM in guanidinium chloride (GdmCl) and in urea, and determined the stability of the enzyme. With these data, together with the information available in the literature, we discuss in detail the possible reasons for the oligomeric nature of TIM.

MATERIALS AND METHODS

Materials

Glycerol-3-phosphate dehydrogenase (GDPH) and GdmCl were from Boehringer–Mannheim, urea from Aldrich. All other reagents were purchased from Sigma. Production, expression and purification of recombinant yTIM were performed as described by Vázquez-Contreras et al. [24]. The concentration of purified yTIM was measured using a molar absorption coefficient (ϵ_{280}) of 26664 $M^{-1} \cdot cm^{-1}$ [25].

Denaturation (N → U) and renaturation (U → N) experiments

In denaturation experiments (N → U), an aliquot of a concentrated yTIM stock solution was diluted in 100 mM triethanolamine, pH 7.4, containing 1 mM EDTA, 0.1 mM dithiothreitol (DTT) (Buffer A) and different concentrations of GdmCl or urea. For the renaturation experiments (U → N), the enzyme was first exposed to 6 M GdmCl for 45 min or 8 M urea for 6 h, conditions under which yTIM is completely unfolded, as indicated by the absence of catalytic activity as well as by CD and intrinsic-fluorescence spectra. These incubation times were enough for the enzyme to reach the unfolded state, since all the monitored properties remained unchanged after 24 h. After this step, renaturation was started by dilution of the unfolded protein in buffer A that contained decreasing concentrations of GdmCl or urea. In both types of experiment, yTIM concentration was in the range 7.5 nM–7.5 μM.

Spectroscopic measurements

Fluorescence measurements were made on an ISS (Champaign, IL, U.S.A.) PC1 spectrofluorimeter. The temperature of the cells was maintained at 25 ± 0.1 °C. Fluorescence measurements were carried out at an excitation wavelength of 280 nm (4 nm bandwidth) and emission was monitored from 300 to 400 nm (8 nm bandwidth). The fluorescence spectral centre of mass (SCM) was calculated from intensity data (I_λ) obtained at different wavelengths using:

$$SCM = \sum \lambda \cdot I_\lambda / \sum I_\lambda$$

CD of yTIM samples (1.85–7.5 μM) was monitored at 222 nm with a JASCO J-715 spectropolarimeter using 0.1-cm-pathlength cells thermostatically maintained at 25 ± 0.1 °C. The values reported were the average of 4 min scans, recorded every 10 s. Reference samples without protein were subtracted in all spectroscopic measurements.

Catalytic-activity measurements

yTIM activity was measured in 1 ml of a mixture that contained 100 mM triethanolamine, pH 7.4, 10 mM EDTA and 1 mM DTT (Buffer B), containing 3.0 mM D,L-glyceraldehyde-3-phosphate, 10 μg of GDPH, 0.2 mM NADH and 75 pM yTIM [26]. Reaction rates were determined from the decrease in absorbance at 340 nm as a function of time in a Beckman DU7500 spectrophotometer with a multicell device thermostatically maintained at 25 ± 0.1 °C. Catalytic-activity measurements are complicated by the presence of high concentrations of denaturants because of their effect on the activity of the coupling enzyme. In addition, TIM catalytic-activity measurements must be carried out at much lower protein concentrations (≈ 1000 times) than those used for spectroscopic measurements. Therefore, activity was measured as follows. Samples (7.5 μM–75 nM yTIM) were first diluted to 7.5 nM without changing the concentration of denaturant. Aliquots were withdrawn from the aforementioned mixture and further diluted in the activity reaction mixture; this procedure took 15 s. After this final dilution step, the yTIM concentration was 75 pM and the residual denaturant concentration was either 60 mM GdmCl or 80 mM urea; The time courses of NADH oxidation were linear, indicating that no re- or de-activation took place during reaction-rate measurements. As previously found, the dilution step did not affect activity values, and control experiments showed that catalytic-activity measurements were not affected by residual concentrations of denaturant in the assay media [23].

Hydrodynamic measurements

Size-exclusion-chromatography experiments were performed on a Superdex 75 HR 10/30 gel-filtration column coupled to a Pharmacia (Uppsala, Sweden) FPLC system. Protein elution was monitored with a Waters 474 scanning fluorescence detector, using an excitation wavelength of 280 nm (18 nm bandwidth), emission being monitored at 320 nm (18 nm bandwidth). The incubated enzymes were loaded on to the filtration column, which had been equilibrated with Buffer B and GdmCl. The samples were eluted at a flow rate of 0.4 ml · min^{-1}. Stokes-radii (R_s) values were calculated from elution volumes and a calibration curve [23,27].

Data fitting

The refolding of the unfolded monomers (U) into the native dimer (N) was analysed according to a three-state model involving a monomeric intermediate (M):

$$2U \underset{}{\overset{K_{fold}}{\rightleftharpoons}} 2M \overset{K_{assoc}}{\rightleftharpoons} N \quad (1)$$

The changes in Gibbs energy for monomer folding (ΔG_{fold}) and monomer association (ΔG_{assoc}), defined as $\Delta G_{fold} = -RT \ln (M/U)$ and $\Delta G_{assoc} = -RT \ln (N/M^2)$ (where R is the gas constant, T is the temperature and ln is logarithm to the base e), were assumed to vary linearly with denaturant concentration x according to:

$$\Delta G_{fold} = \Delta G^0_{fold} + m_{fold} x \quad (2)$$

$$\Delta G_{assoc} = \Delta G^0_{assoc} + m_{assoc} x \quad (3)$$

where m is the dependence of free energy on denaturant concentration. The molar fractions of subunits in the unfolded, monomeric and native states are defined by $f_U = U/P_t$, $f_M = M/P_t$ and $f_N = 2N/P_t$ respectively, where the total protein concentration (P_t) is expressed on a monomer basis ($P_t = U + M + 2N$). f_M and f_N can be expressed as a function of the equilibrium constants as:

$$f_M = \frac{-\left(\frac{1}{K_{fold}} + 1\right) + \sqrt{\left(\frac{1}{K_{fold}} + 1\right)^2 + 8K_{assoc}P_t}}{4K_{assoc}P_t} \quad (4)$$

$$f_N = 2(f_M)^2 \cdot K_{assoc} \cdot P_t \quad (5)$$

with $f_U = 1 - f_N - f_M$. In obtaining eqns (4) and (5), the experimental observable (y) was assumed to be additive $y = y_U f_U + y_M f_M + y_N f_N$. In order to compare and use data from different techniques, it is convenient to normalize the experimental values as $\alpha = [y(x) - y(x')]/[y(x = 0) - y(x')]$, where x' is

the denaturant concentration for complete unfolding. The parameters ΔG^0_{fold}, m_{fold}, ΔG^0_{assoc} and m_{assoc} were fitted to $\alpha(x)$ using eqns (4) and (5).

RESULTS AND DISCUSSION

Unfolding and refolding of yTIM

yTIM was incubated in 6 M GdmCl or in 8 M urea. Incubation times longer than 10 min in GdmCl or 5 h in urea leads to complete unfolding of yTIM, as indicated by the complete inactivation of the enzyme, a far-UV CD spectrum characteristic of unfolded proteins, a decrease in the quantum yield of the fluorescence spectrum and a red shift in the SCM to 351 nm (results not shown). In what follows, yTIM incubated for 45 min in 6 M GdmCl or for 6 h in 8 M urea was used as the unfolded (U) starting material for the U → N experiments. The spectroscopic and catalytic properties of yTIM were determined after different incubation times in the U → N experiments (Figure 1, closed symbols) and in the conventional N → U experiments (Figure 1, open symbols). The fluorescence and catalytic activity of yTIM at concentrations below 0.5 M GdmCl or 1.0 M urea were native-like in both the N → U and U → N samples. The latter indicates that yTIM renaturation is fully reversible. N → U and U → N samples were inactive and showed a similar SCM at high concentrations of denaturants (1.5–2.5 M GdmCl or 7.0–8.0 M urea). At these low and high denaturant concentrations, both types of experiments gave the same results. In contrast, there were differences in the N → U and U → N courses at intermediate concentrations of denaturant (Figure 1). While the spectroscopic and functional properties of yTIM in the U → N samples reached a constant value after 48 h in both GdmCl and urea (closed symbols in Figure 1), in the N → U experiments (open symbols in Figure 1) there was a very slow change in the SCM and catalytic activity towards the values observed in the U → N direction. The data in Figure 1 indicate that, in the U → N experiments, equilibrium was truly reached, while in the N → U experiments this was not the case. The hysteresis observed in Figure 1 after incubation for conventional (1 or 2 days) and much higher 'equilibrium times' was probably due to slow kinetics of the dissociation and/or the unfolding transition(s).

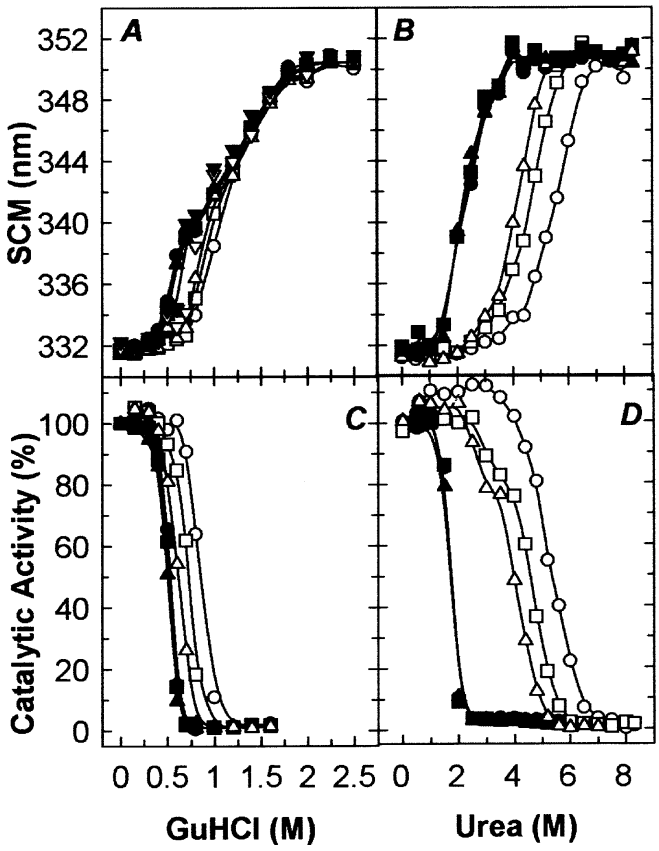

Figure 1 Hysteresis between the unfolding (N → U) and refolding (U → N) of yTIM

yTIM samples (0.75 μM) from N → U (open symbols) and U → N (closed symbols) experiments were monitored by the SCM of the fluorescence spectra (**A** and **B**) or catalytic activity (**C** and **D**). Measurements were taken after incubation for 96 (○, ●), 168 (□, ■) and 240 (△, ▲) h in GdmCl ('GuHCl') (**A** and **C**) or 48 (○, ●), 192 (□, ■) and 360 (△, ▲) h in urea (**B** and **D**). Lines are drawn to aid visualization.

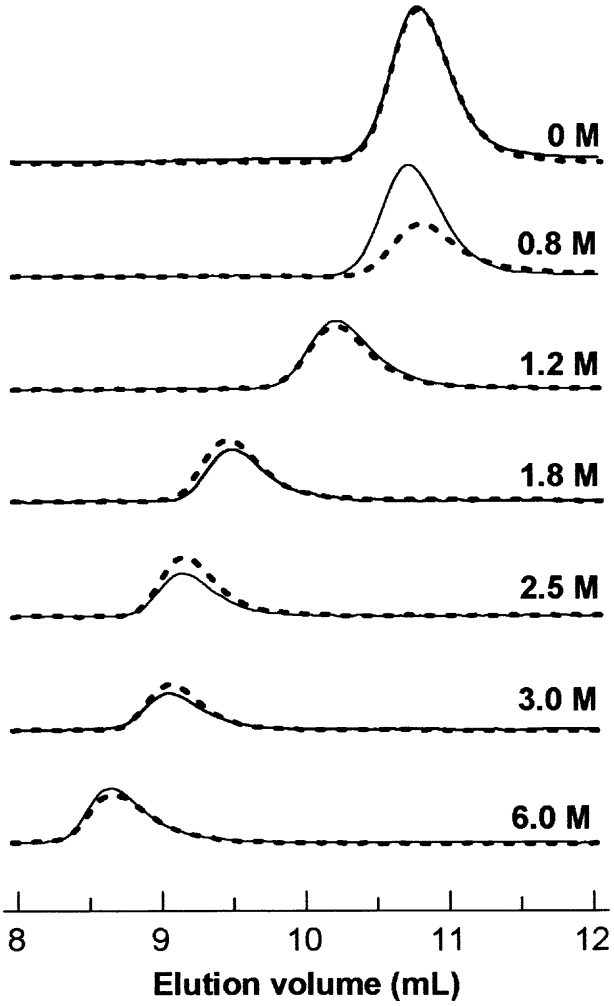

Figure 2 Elution profiles of yTIM from N → U and U → N experiments in the presence of GdmCl

yTIM samples (0.75 μM) from N → U (continuous lines) and U → N (broken lines) experiments were incubated for 24 h in the presence of GdmCl; thereafter samples (100 μl) were injected into a Superdex 75 column equilibrated in the same concentration of denaturant. Elution profiles were monitored by fluorescence intensity ($\lambda_{excitation}$ = 280 nm; $\lambda_{emission}$ = 320 nm).

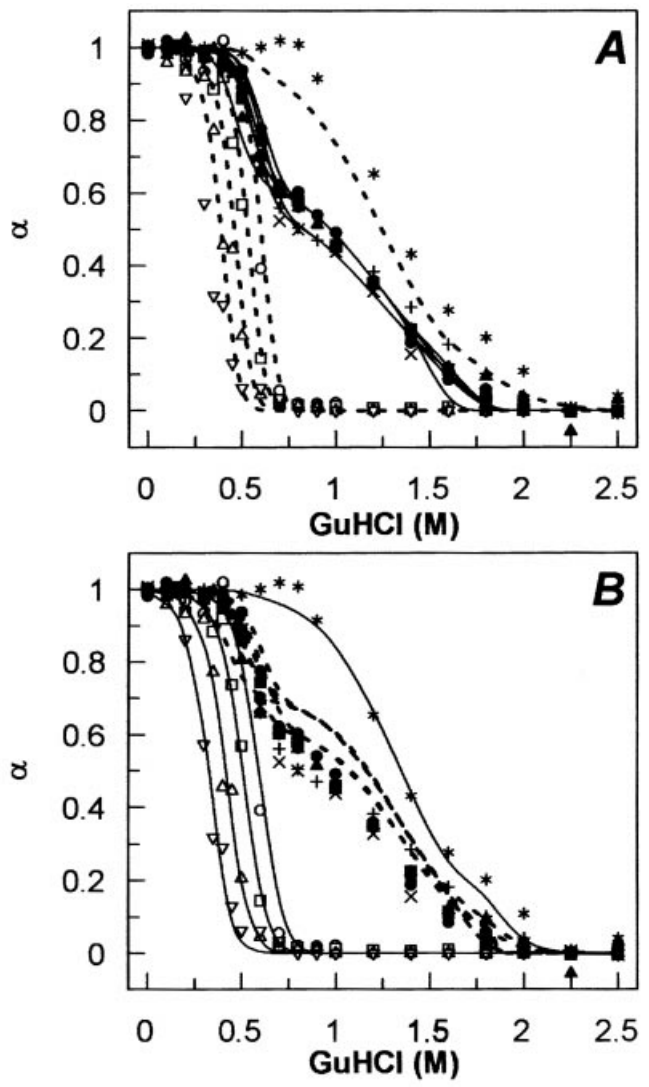

Figure 3 Three-state analysis of yTIM renaturation (U → N) in the presence of GdmCl ('GuHCl')

Normalized changes for yTIM renaturation experiments (U → N) in GdmCl followed by SCM at 7.5 (●), 1.85 (⬢), 0.75 (■) and 0.075 (▲) μM, CD at 7.5 (+) and 1.85 (×) μM, catalytic activity at 7.5 (○), 0.75 (□), 7.5^{-2} (△) and 7.5^{-3} (▽) μM and R_s at 0.75 μM (*). In each panel, continuous lines are fits to eqns (4) and (5); broken lines are predictions. Parameters obtained using alternative (*i*) (**A**) and alternative (*ii*) (**B**) are given in Table 1.

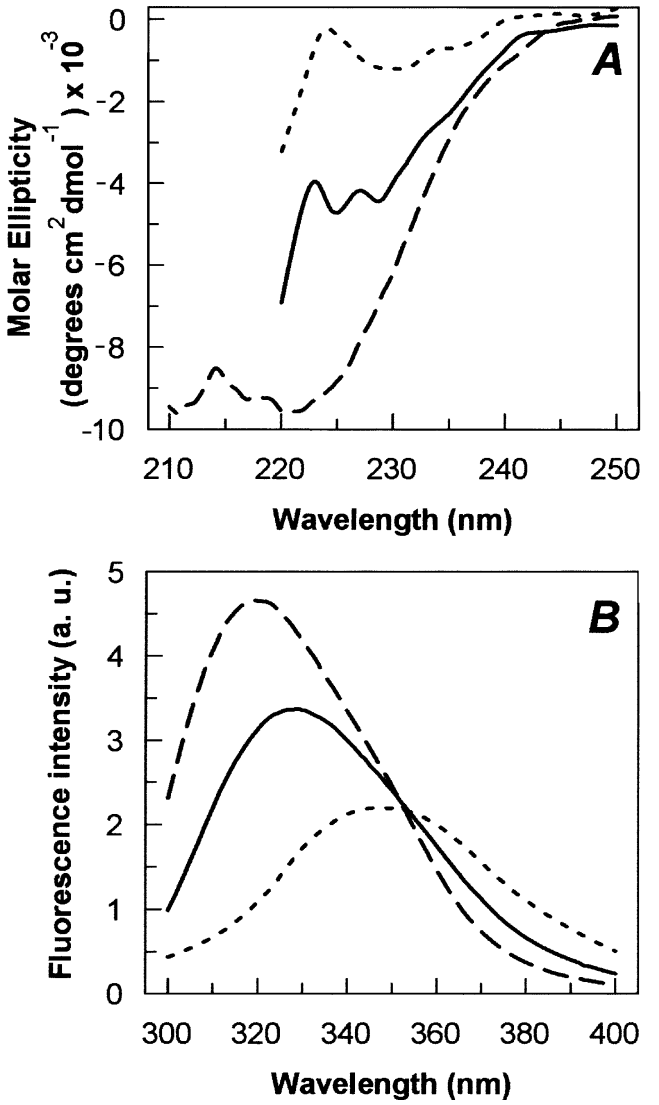

Figure 4 Spectroscopic properties of the three states of yTIM observed in U → N experiments

Far-UV CD (**A**) and fluorescence (**B**) spectra of yTIM were obtained at 0 (long-dash broken lines), 0.7 (continuous lines) and 2.5 (short-dash broken lines) M GdmCl. According to the three-state analysis (see the text), the maximum concentration of intermediate ($f_M = 0.92$) was estimated to occur at 0.7 M GdmCl.

The hydrodynamic properties of yTIM in the presence of GdmCl were explored using size-exclusion chromatography [23,27]. A single elution peak was observed at all the GdmCl concentrations tested (Figure 2). The R_s of yTIM shows an increase in going from 0 to 6 M GdmCl from 30.0 to 44.9 Å (1 Å = 0.1 nm) (Figure 2). The R_s of unfolded yTIM varied between 40.9 and 44.9 Å in going from 2.5 to 6.0 M GdmCl (Figure 2). The elution profiles of yTIM samples in the N → U and U → N courses were similar at low (0–0.4 M GdmCl) and high concentrations (1.2–6.0 M GdmCl) of denaturant (Figure 2). However, in 0.8 M GdmCl the elution profiles of yTIM clearly differed in quantum yield (Figure 2). In spite of this difference in fluorescence properties, the R_s of yTIM in N → U and U → N experiments are coincident at all the times (24, 96 and 168 h) and GdmCl concentrations studied.

In an effort to find conditions for coincidence between the N → U and U → N experiments, both courses were also studied at 30 °C, where faster kinetics would be expected. The properties of U → N samples remained almost unchanged after 48 h (results not shown). As observed at 25 °C, the N → U samples at 30 °C progressively reached the U → N values. It was after 10 days that coincidence was achieved (results not shown), i.e. within a shorter time than at 25 °C. However, at 30 °C and this long incubation time, a decrease in the catalytic activity and a red shift in the SCM values were also observed in the native enzyme and in the U → N experiments. Since it is known that long incubation times or relatively high temperatures promote collateral chemical reactions between the protein and denaturants, as well as protein degradation [28–30], no further experiments were carried out at 30 °C.

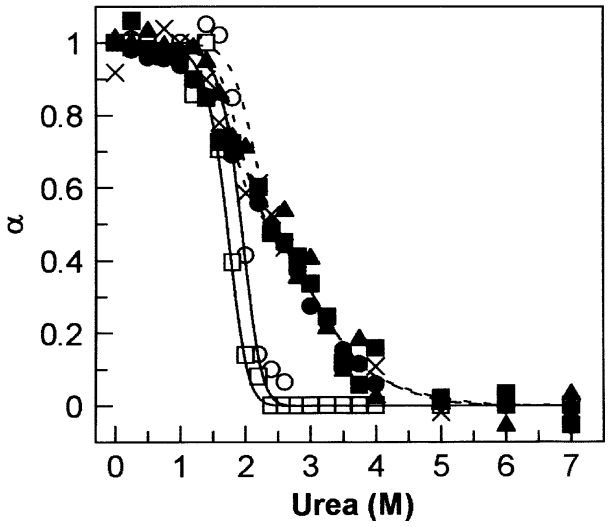

Figure 5 Three-state analysis of yTIM renaturation (U → N) in the presence of urea

Normalized changes for yTIM renaturation experiments (U → N) in urea followed by SCM at 7.5 (●), 0.75 (■) and 0.225 (▲) μM, CD at 7.5 (×) μM and catalytic activity at 2.25 (○) and 0.225 (□) μM. Continuous lines (catalytic activity) and broken lines (CD and SCM) are fits to eqns (4) and (5). Parameters are reported in Table 1 (alternative *iv*).

An equilibrium intermediate in the refolding of yTIM

On the basis of the above findings, hereafter only the results of U → N experiments at 25 °C are analysed. To facilitate the analysis and comparison of results using different techniques, results are henceforth expressed in their normalized form $\alpha(x)$ (see above). The intrinsic fluorescence and CD of yTIM in the presence of GdmCl exhibited two transitions (Figure 3), indicating the presence of an intermediate. The first transition, observed at high concentrations of denaturant (between 2.5 and 1.0 M GdmCl), is characterized by partial burial of aromatic residues and secondary-structure formation. A shoulder was detected from 1.0 to 0.6 M. In the second transition, observed at GdmCl concentrations lower than 0.6 M, yTIM acquired the spectral properties and secondary structure of the native enzyme. yTIM was inactive in the region that corresponds to the first transition detected by the spectroscopic techniques. Catalytic activity appeared in the second transition, indicating that the intermediate is inactive (Figure 3). The R_s of yTIM was native-like in the second transition, so the intermediate might be a native-like dimer or an expanded monomer. Since yTIM is a dimer, its refolding must include a bimolecular step, and hence the association state of the intermediate can be determined from the effect of protein concentration on the transitions. The dependence of $\alpha(x)$ on protein concentration has been considered to be the best criterion for assigning the bimolecular step in a folding mechanism ([8] and references therein). Variations in yTIM concentration had no clear effect on the transitions detected by spectroscopic or hydrodynamic measurements (results not shown). However, as the yTIM concentration was decreased, the re-activation curves were displaced to lower denaturant concentration (Figure 3). Therefore, the second transition is a bimolecular reaction, where inactive monomers associate to form the active dimer. The spectroscopic properties of the three states are shown in Figure 4. It is seen that the intermediate possesses a considerable amount of secondary structure, whereas its fluorescence spectra shows that aromatic residues are partially buried, final rearrangements in their environment being accomplished upon association. Similar spectra were reported for N → U experiments [22].

Although dimers and monomers are in equilibrium in the second transition, the R_s of yTIM remained constant (Figure 3) and a single elution peak was observed (Figure 2). This may reflect the average of two states with different hydrodynamic properties in fast equilibrium, or that the hydrodynamic properties of the monomeric intermediate and the native dimer are similar. Because the approach to equilibrium is extremely slow (Figures 1A and 1C), the first possibility was ruled out. Therefore, the native dimer and the monomeric intermediate have similar R_s values (30 Å) and the latter is therefore more expanded than the 'native monomer' in the dimer. From NMR experiments, the hydrodynamic radii (R_h) for native yTIM and for the monomeric intermediate observed in unfolding experiments are 24 and 29.6 Å respectively [22]. The intermediate described here is less expanded than the monomeric intermediate observed in the unfolding of the TIM from *Trypanosoma brucei* (TbTIM) (R_s = 36 Å) [23] and the two unfolding intermediates of the α-subunit of tryptophan synthase (R_s = 37.9 and 52.9 Å), which is a monomeric β/α barrel protein of a similar molecular mass (27 kDa) [31].

In urea, the presence of an intermediate is clearly indicated by the non-coincidence of activity and spectroscopic data. Despite this, only a rather weak shoulder around 2.5 M urea was detected by CD and SCM (Figure 5). yTIM was inactive in the first transition, between 7.0 and 2.5 M urea, and re-activates at denaturant concentrations that correspond to the second transition (less than 2.5 M urea). As with GdmCl, enzyme re-activation depended on protein concentration (Figure 5). These data strongly suggest that the same three-state mechanism observed for the enzyme in GdmCl is also present for the enzyme in urea. In order to explore the effect of ionic strength on the equilibrium reassociation of yTIM, we measured the effect of moderate NaCl concentrations (0.3 and 0.6 M) on the activity profile in urea. Within experimental error, no changes were detected in the presence of NaCl (results not shown).

Calculation of yTIM stability

The simplest model accounting for the present data is a three-state model $2U \rightleftharpoons 2M \rightleftharpoons N$, where the unfolded monomers partially fold into expanded and inactive monomers which further assemble into the native active dimer. Since U → N experiments reached equilibrium, these were used to calculate the Gibbs energy changes associated with the observed transitions, i.e. monomer folding (ΔG_{fold}) and monomer association (ΔG_{assoc}). Given that for yTIM there are data for two denaturants and several techniques, it is possible to use different sets of data to obtain the thermodynamic parameters whose values, in principle, should be independent of the chosen data set. Furthermore, it is possible to use a subset of values and predict, with the ΔG^0_{fold} and ΔG^0_{assoc} obtained, the behaviour of another set. This allows us to test the internal consistency of the data and the soundness of the proposed model, and to evaluate the physical reliability of the obtained values for the parameters. In this framework, ΔG^0_{fold} and ΔG^0_{assoc} were evaluated for five alternatives. In all these fittings, the normalized signal for the unfolded monomer $y_U = 0$ and for the native dimer $y_N = 1$, while in accordance with the discussion in the previous subsection, for activity data the normalized signal for the monomeric intermediate $y_M = 0$ and for hydrodynamic data $y_M = 1$. In the first alternative (*i*), the thermodynamic parameters were fitted to fluorescence and CD data in GdmCl, predicting catalytic activity and hydrodynamic

Table 1 Stability of yTIM at 25 °C and pH 7.4

	Gibbs energy change (kJ · mol^{-1})		
Fit	ΔG^0_{fold}	ΔG^0_{assoc}	ΔG^0_{tot}
(*i*)*	-10.49 ± 0.79	-77.48 ± 0.89	-98.46
(*ii*)†	-16.38 ± 1.46	-67.59 ± 0.82	-100.35
(*iii*)‡	-15.91 ± 0.05	-68.01 ± 0.31	-96.42
(*iv*)§	-12.41 ± 1.38	-83.26 ± 1.92	-108.08
(*v*)¶	-16.59 ± 0.71	-70.26 ± 1.08	-103.44

* y_M (CD) $= 0.64 \pm 0.02$ and y_M (SCM) $= 0.71 \pm 0.02$ used as fitting parameters.
† y_M (CD) and y_M (SCM) were taken as constants equal to those obtained in alternative (*i*).
‡ y_M (CD) $= 0.55 \pm 0.02$ and y_M (SCM) $= 0.63 \pm 0.01$ used as fitting parameters.
§ y_M (CD and SCM) $= 0.68$ was taken as constant equal to the average of those obtained in alternative (*i*).
¶ y_M (CD) $= 0.52 \pm 0.03$ and y_M (SCM) $= 0.59 \pm 0.02$ used as fitting parameters.

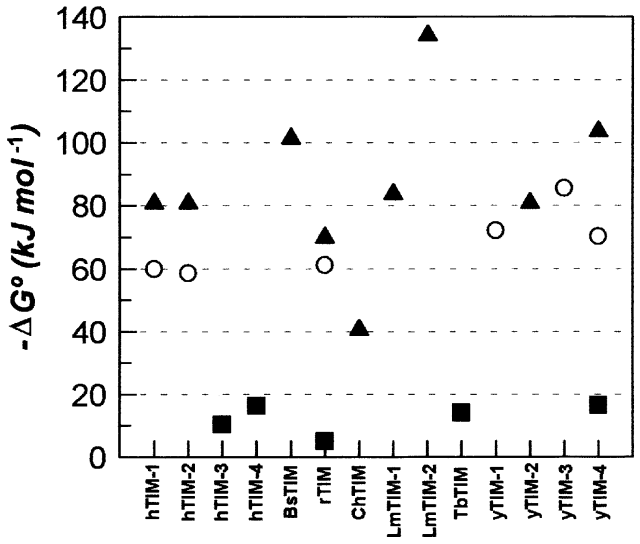

Figure 6 Stability of TIM from different species

Unless otherwise stated, data are for wild-type enzymes at 25 °C and pH 7.4. ΔG^0_{fold} (■), ΔG^0_{assoc} (○) and ΔG^0_{tot} (▲). The code for the labels on the abscissa is as follows: hTIM-1, human TIM at pH 8.0 [5]; hTIM-2, ΔG^0_{assoc} from [5] and ΔG^0_{tot} from [18]; hTIM-3, M14Q/R98Q monomeric mutant [5,18]; hTIM-4, M14Q/R98Q/Q179D/K193A/A215P monomeric mutant [18]; BsTIM, *Bacillus stearothermophilus* TIM [18]; rTIM, rabbit TIM [19]; ChTIM, chicken TIM at 30.4 °C [34]; LmTIM-1, *Leishmania mexicana* TIM at pH 7.5 [21]; LmTIM-2, E65Q mutant at pH 7.7 [21]; TbTIM, *Trypanosoma brucei* TIM monomeric mutant at pH 6.8 [21]; yTIM-1, *Saccharomyces cerevisiae* TIM average ΔG^0_{assoc} at pH 7.2 [22]; yTIM-2, ΔG^0_{tot} from thermal denaturation extrapolated to 25 °C [17]; yTIM-3, average ΔG^0_{assoc} calculated from structural data and solvation parameters [35]; and yTIM-4, the present work (Table 1, alternative *v*).

data. In the second alternative (*ii*) the converse was done, i.e. parameters were fitted to catalytic-activity and hydrodynamic data and the spectroscopic behaviour was predicted. The ΔG^0 obtained for alternatives (*i*) and (*ii*) are given in Table 1, their predictive power being displayed in Figure 3. In alternative (*i*) (Figure 3A), the spectroscopic signal of the monomer (y_M) was also used as a fitting parameter. In alternative (*ii*) (Figure 3B), these two values were used as constants to predict the spectroscopic behaviour. In both cases, the change of $\alpha(x)$ with protein concentration is well reproduced. The third alternative (*iii*) consisted in using all the available data in GdmCl, again using y_M for spectroscopic data as an adjustable parameter, the resulting ΔG^0 being reported in Table 1. For urea, alternatives (*i*) and (*ii*) were not considered, since, as mentioned above, in this denaturant the biphasic behaviour of the spectroscopic data is less marked and, moreover, hydrodynamic data are not available. Therefore, alternative (*iv*) used all the available data in urea. Here, the spectroscopic signal of the intermediate is difficult to obtain as a fitted parameter and hence the y_M value obtained in the analysis of GdmCl data (alternative *i*) was used as a fixed parameter (Table 1). Finally, alternative (*v*) was a global fit employing all the available data in both denaturants and using the values of y_M (SCM) and y_M (CD) as adjustable parameters. In Table 1, the fitted spectroscopic y_M values are between 0.52 and 0.71, indicating that in comparison with the native dimer, the monomeric intermediate contains substantial secondary structure and the aromatic residues are partially buried, as observed in the spectroscopic data shown in Figure 4. The ΔG^0_{fold} and ΔG^0_{assoc} values obtained from the five alternatives are close, and, for all of them, $\Delta G^0_{assoc} \gg \Delta G^0_{fold}$. The large magnitude of ΔG^0_{assoc} is in agreement with dilution experiments, since, after a 3-month incubation time, the catalytic activity of yTIM remained constant and independent of enzyme concentration over the range from 75 pM to 7.5 μM (see below). The comparison among alternatives (*iii*)–(*v*) suggests that the folding and association of yTIM is thermodynamically equivalent in both denaturants. As observed previously for other proteins, the *m* values for GdmCl are considerably larger than those for urea. Since the data employed in alternatives (*i*)–(*v*) are all at equilibrium, the small differences seen in Table 1 can be attributed to experimental error. From this point of view, the results of the global fit (alternative *v*) must be the most satisfactory, since in this fitting some of these experimental inaccuracies are compensated for.

Unfolding of TIM from different species and other β/α barrels

The unfolding of TIM has been extensively studied, but, often, irreversibility has been observed [20,23,32,33]. Figure 6 displays all the available data regarding the thermodynamic stability of TIM from different species [5,17–19,21,22,34]. In contrast with the present data for yTIM, where biphasic behaviour was detected and used to obtain the Gibbs energy changes, in all other cases, monophasic transitions were employed using a two-state model ($2U \rightleftharpoons N$). Therefore, the only reported Gibbs energy changes involving an intermediate had to be obtained from kinetic data for rTIM [19] or from the unfolding of monomeric mutants of human TIM (hTIM) [5,18] and of TbTIM [21]. All thermodynamic characterizations of TIM stability in Figure 6 have used experiments in the $N \rightarrow U$ direction or calculations from structural data [35]. In this respect, the results in Figure 1 clearly show that caution must be exercised when using only data from $N \rightarrow U$ experiments to obtain thermodynamic parameters, since, unless long incubation times are employed, equilibrium might not have been reached. Despite the different conditions used to obtain the data in Figure 6, for all TIM species there is a clear relation between the Gibbs energy changes for the association and folding transitions, namely ΔG_{assoc} is much bigger than ΔG_{fold}. The fractional contribution of monomer folding to the stability of the native enzyme (estimated as $2\Delta G^0_{fold}/\Delta G^0_{tot}$) varies between 0.14 for rTIM to 0.32 for yTIM; that is, subunit assembly notably increases the conformational stability of TIM, as previously stated [5]. In all cases monomer folding is a favourable process, the ΔG_{fold} values obtained for wild-type TIMs varying from -5.0 to -16.6 kJ · mol^{-1}. This indicates that TIM monomers are marginally stable. Since these values are smaller than those observed for the folding of monomeric proteins [36], it can be concluded that TIM is dimeric, mainly because of stability considerations [5]. In contrast, other approaches (see below)

suggest that the high catalytic skills of TIM are linked to the oligomeric nature of the enzyme. In what follows, through the comparison between TIM results and those obtained for other β/α barrels, we analyse the relative contributions of stability and function as reasons for the dimeric nature of TIM.

The stability hypothesis is based on two underlying assumptions. First, that monomeric and active β/α barrels with low stability are not likely to occur. Secondly, that, in the absence of quaternary interactions, high stability cannot be achieved for β/α barrels. The first assumption is not in agreement with the low stability reported for the monomeric and active aldolase from *Staphylococcus aureus* ($\Delta G^0_{fold} = -9.0 \pm 2.0$ kJ · mol^{-1}) [37]. Regarding the second assumption, a highly stable β/α barrel, namely the α-subunit of tryptophan synthase, has been reported; in this case, $\Delta G^0_{tot} = -34.3$ and -64.42 kJ · mol^{-1} from the GdmCl- and urea-induced unfolding respectively [38,39]. Therefore the stability range for monomeric and active β/α barrels is very broad (-9 to -64 kJ · mol^{-1}); moreover, it varies significantly with pH, as observed in the indol-3-ylglycerol phosphate synthase from *Sulfolobus solfataricus*, where ΔG^0_{fold} changes from -14.7 ± 1.2 kJ · mol^{-1} at pH 7.0 to -25.5 ± 1.8 kJ · mol^{-1} at pH 9.0 [40]. The stability of yTIM monomers obtained in this work (-16.6 ± 0.7 kJ · mol^{-1}; Table 1) is clearly within this range, but closer to the lower limit. Noticeably, the stability of monomeric β/α barrels can be increased, as shown by the results for hTIM monomeric mutants, where the stability increased from -10.46 to -16.32 kJ · mol^{-1} [18]. It is clear, then, that there are examples that undermine the validity of the two above-mentioned assumptions. On the other hand, the functional hypothesis finds strong support from the fact that, despite the significant research efforts made so far, the catalytic activity of monomeric TIM mutants is at best 100 times lower than that of wild-type TIMs [41,42]. This is remarkable, considering that active-site residues are self-contained in the monomer. It has been proposed that the huge increase in catalytic activity observed upon association is due to intersubunit contacts that decrease the flexibility of the catalytic loops [6]. In the case of yTIM, the intersubunit contacts occurring during reassociation involve adjustments in the secondary and tertiary structure (Figure 4), as well as monomer shrinking. Other approaches, such as refolding kinetics in conventional and low-water media, as well as stability towards dilution [43–47], indicate that TIM catalysis requires dimerization.

Some insight might be gained by the analysis of the fraction of active TIM as a function of protein concentration. These experimental data are shown in Figure 7, together with the prediction using the ΔG^0 values obtained in the present study using the three-state model described above (Table 1, alternative *v*). Figure 7 also shows three simulations for different ΔG^0 values. The first two simulations indicate that activity is practically constant when $\Delta G^0_{assoc} = -70$ kJ · mol^{-1}, and ΔG^0_{fold} is changed from 0 to -70 kJ · mol^{-1}; that is, from a non-stable to very stable monomer. In other words, the activity profile is almost independent of ΔG^0_{fold}. In the third simulation, ΔG^0_{assoc} was reduced by half (-35 kJ · mol^{-1}) while maintaining a very stable monomer ($\Delta G^0_{fold} = -75$ kJ · mol^{-1}), the result being that catalytic activity is drastically reduced. Since *in vivo* TIM concentrations for different species are between 1×10^{-5} and 1×10^{-6} M [48] and monomers are barely active, it is clear from Figure 7 that a high ΔG^0_{assoc} is needed for catalysis. It is likely that there is no evolutionary pressure that favours the appearance of stable monomers. The possibility that a stable dimer formed early in evolution and was subsequently optimized for perfect catalysis should be considered. From the above discussion it appears that the available data for TIM indicates that there is not a unique

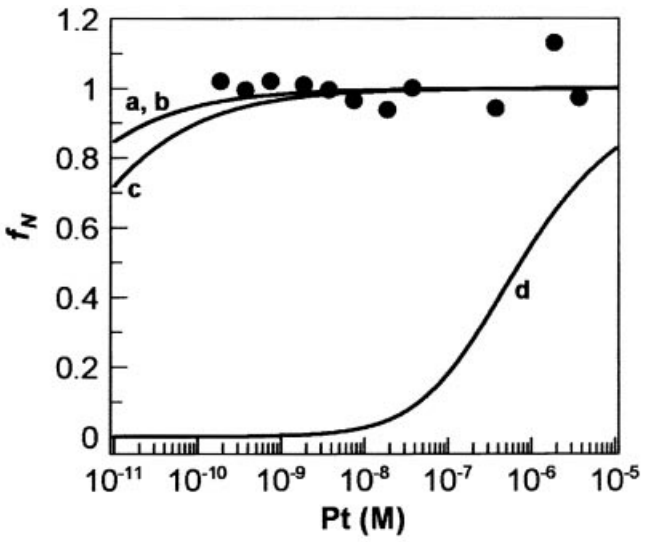

Figure 7 Fraction of active yTIM molecules as a function of protein concentration [P_t ('Pt')]

Experimental data for the fraction of native molecules as a function of yTIM concentration (●) are compared with simulations based on the following values of ΔG^0_{fold} and ΔG^0_{assoc} (in kJ · mol^{-1}) respectively: trace a, -16.6 and -70.3 (from Table 1, alternative *v*); b, -70 and -70; trace c, 0 and -70; and trace d, -75 and -35. Traces a and b are indistinguishable.

reason for the dimeric nature of TIM. For oligomeric proteins, function and stability are intimately linked. Hence, the dimeric nature of TIM should be examined in the light of this interplay. Definitively the low stability of TIM monomers is neither the only, nor the main, cause.

It would be valuable to widen the present discussion to include oligomers of different fold types. The data in [8,49–52] indicate that, in many cases, the stability of the dimer contributes significantly to the conformational free energy of the protein, as discussed above for TIM. However, since there are relatively few thermodynamic studies for the dissociation/association of oligomeric proteins, general conclusions are difficult to make.

We thank Professor M. Calcagno, Professor A. Gómez-Puyou, Professor A. Hernández-Arana and Professor R. A. Muñoz-Clares for helpful discussions, Professor V. Donhal for his advice on the fitting procedures and Dr M. E. Chánez-Cardenas for her help with the FPLC experiments. This work was partially supported by a grant from the Consejo Nacional de Ciencia y Tecnología (CONACyT) (34815-N, 27986-E). H. N. was a recipient of Programa de Apoyo a las Divisiones de Estudios de Postgrado-Universidad Nacional Autónoma de México (PADEP-UNAM) and CONACyT scholarships.

REFERENCES

1 Jaenicke, R. (1987) Folding and association of proteins. Prog. Biophys. Mol. Biol. **49**, 117–237
2 Traut, T. W. (1994) Dissociation of enzyme oligomers: a mechanism for allosteric regulation. Crit. Rev. Biochem. Mol. Biol. **29**, 125–163
3 Farber, G. K. and Petsko, G. A. (1990) The evolution of α/β barrel enzymes. Trends Biochem. Sci. **15**, 228–234
4 Copley, R. R. and Bork, P. (2000) Homology among $(\beta\alpha)_8$ barrels: implications for the evolution of metabolic pathways. J. Mol. Biol. **303**, 627–641
5 Mainfroid, V., Terpstra, P., Beauregard, M., Frère, J. M., Mande, S. C., Hol, W. G., Martial, J. A. and Goraj, K. (1996) Three hTIM mutants that provide new insights on why TIM is a dimer. J. Mol. Biol. **257**, 441–456
6 Schliebs, W., Thanki, N., Jaenicke, R. and Wierenga, R. K. (1997) A double mutation at the tip of the dimer interface loop of triosephosphate isomerase generates active monomers with reduced stability. Biochemistry **36**, 9655–9662

7 Bowie, J. U. and Sauer, R. T. (1989) Equilibrium dissociation and unfolding of the Arc repressor dimer. Biochemistry **28**, 7139–7143
8 Neet, K. E. and Timm, D. E. (1994) Conformational stability of dimeric proteins: quantitative studies by equilibrium denaturation. Protein Sci. **3**, 2167–2174
9 Jaenicke, R. and Lilie, H. (2000) Folding and association of oligomeric and multimeric proteins. Adv. Protein Chem. **53**, 329–401
10 Baker, D., Sohl, J. L. and Agard, D. A. (1992) A protein-folding reaction under kinetic control. Nature (London) **356**, 263–265
11 Sinclair, J. F., Ziegler, M. M. and Baldwin, T. O. (1994) Kinetic partitioning during protein folding yields multiple native states. Nat. Struct. Biol. **1**, 320–326
12 Lai, Z., McCulloch, J., Lashuel, H. A. and Kelly, J. W. (1997) Guanidine hydrochloride-induced denaturation and refolding of transthyretin exhibits a marked hysteresis: equilibria with high kinetic barriers. Biochemistry **36**, 10230–10239
13 Rosengarth, A., Rösgen, J. and Hinz, H. J. (1999) Slow unfolding and refolding kinetics of the mesophilic Rop wild-type protein in the transition range. Eur. J. Biochem. **264**, 989–995
14 Engel, J. and Bächinger, H. P. (2000) Cooperative equilibrium transitions coupled with a slow annealing step explain the sharpness and hysteresis of collagen folding. Matrix Biol. **19**, 235–244
15 Zhu, L., Fan, Y. X. and Zhou, J. M. (2001) Identification of equilibrium and kinetic intermediates involved in folding of urea-denatured creatine kinase. Biochim. Biophys. Acta **1544**, 320–332
16 Rietveld, A. W. and Ferreira, S. T. (1998) Deterministic pressure dissociation and unfolding of triosephosphate isomerase: persistent heterogeneity of a protein dimer. Biochemistry **37**, 933–937
17 Benítez-Cardoza, C. G., Rojo-Domínguez, A. and Hernández-Arana, A. (2001) Temperature-induced denaturation and renaturation of triosephosphate isomerase from *Saccharomyces cerevisiae*: evidence of dimerization coupled to refolding of the thermally unfolded protein. Biochemistry **40**, 9049–9058
18 Mainfroid, V., Mande, S., Hol, W., Martial, J. and Goraj, K. (1996) Stabilization of human triosephosphate isomerase by improvement of the stability of individual α-helices in dimeric as well as monomeric forms of the protein. Biochemistry **35**, 4110–4117
19 Rietveld, A. W. and Ferreira, S. T. (1996) Kinetics and energetics of subunit dissociation/unfolding of TIM: the importance of oligomerization for conformational persistence and chemical stability of proteins. Biochemistry **35**, 7743–7751
20 Gokhale, R. S., Ray, S. S., Balaram, H. and Balaram, P. (1999) Unfolding of *Plasmodium falciparum* triosephosphate isomerase in urea and guanidinium chloride: evidence for a novel disulfide exchange reaction in a covalently cross-linked mutant. Biochemistry **38**, 423–431
21 Lambeir, A. M., Backmann, J., Ruiz-Sanz, J., Filimonov, V., Nielsen, J. E., Kursula, I., Norledge, B. V. and Wierenga, R. K. (2000) The ionization of a buried glutamic acid is thermodynamically linked to the stability of *Leishmania mexicana* triosephosphate isomerase. Eur. J. Biochem. **267**, 2516–2524
22 Morgan, C. J., Wilkins, D. K., Smith, L. J., Kawata, Y. and Dobson, C. M. (2000) A compact monomeric intermediate identified by NMR in the denaturation of dimeric triosephosphate isomerase. J. Mol. Biol. **300**, 11–16
23 Chánez-Cárdenas, M. E., Fernández-Velasco, D. A., Vázquez-Contreras, E., Coria, R., Saab-Rincón, G. and Pérez-Montfort, R. (2002) Unfolding of triosephosphate isomerase from *Trypanosoma brucei*: identification of intermediates and insight into the denaturation pathway using tryptophan mutants. Arch. Biochem. Biophys. **399**, 117–129
24 Vázquez-Contreras, E., Zubillaga, R., Mendoza-Hernández, G., Costas, M. and Fernández-Velasco, D. A. (2000) Equilibrium unfolding of yeast triosephosphate isomerase: a monomeric intermediate in guanidine-HCl and two-state behaviour in urea. Protein Peptide Lett. **7**, 57–64
25 Norton, I. L. and Hartman, F. C. (1972) Triosephosphate isomerase from bakers' yeast. Preliminary crystallographic data. Biochemistry **11**, 4435–4441
26 Rozacky, E. E., Sawyer, T. H., Barton, R. A. and Gracy, R. W. (1971) Studies on human triosephosphate isomerase. I. Isolation and properties of the enzyme from erythrocytes. Arch. Biochem. Biophys. **146**, 312–320
27 Uversky, V. N. (1993) Use of fast protein size-exclusion liquid chromatography to study the unfolding of proteins which denature through the molten globule. Biochemistry **32**, 13288–13298
28 Stark, G. R. (1965) Reactions of cyanate with functional groups of proteins. IV. Inertness of aliphatic hydroxyl groups. Formation of carbamyl- and acylhydantoins. Biochemistry **4**, 2363–2367
29 Hagel, P., Gerding, J. J., Fieggen, W. and Bloemendal, H. (1971) Cyanate formation in solutions of urea. I. Calculation of cyanate concentrations at different temperature and pH. Biochim. Biophys. Acta **243**, 366–373
30 Gerding, J. J., Koppers, A., Hagel, P. and Bloemendal, H. (1971) Cyanate formation in solutions of urea. II. Effect of urea on the eye lens protein γ-crystallin. Biochim. Biophys. Acta **243**, 375–379
31 Gualfetti, P. J., Iwakura, M., Lee, J. C., Kihara, H., Bilsel, O., Zitzewitz, J. A. and Matthews, C. R. (1999) Apparent radii of the native, stable intermediates and unfolded conformers of the α-subunit of tryptophan synthase from *E. coli*, a TIM barrel protein. Biochemistry **38**, 13367–13378
32 Alvarez, M., Zeelen, J. P., Mainfroid, V., Rentier-Delrue, F., Martial, J. A., Wyns, L., Wierenga, R. K. and Maes, D. (1998) Triosephosphate isomerase (TIM) of the psychrophilic bacterium *Vibrio marinus*. Kinetic and structural properties. J. Biol. Chem. **273**, 2199–2206
33 Beaucamp, N., Hofmann, A., Kellerer, B. and Jaenicke, R. (1997) Dissection of the gene of the bifunctional PGK–TIM fusion protein from the hyperthermophilic bacterium *Thermotoga maritima*: design and characterization of the separate triosephosphate isomerase. Protein Sci. **6**, 2159–2165
34 McVittie, J. D., Esnouf, M. P. and Peacocke, A. R. (1977) The denaturation–renaturation of chicken-muscle triosephosphate isomerase in guanidinium chloride. Eur. J. Biochem. **81**, 307–315
35 Lolis, E., Alber, T., Davenport, R. C., Rose, D., Hartman, F. C. and Petsko, G. A. (1990) Structure of yeast triosephosphate isomerase at 1.9-Å resolution. Biochemistry **29**, 6609–6618
36 Pace, C. N. (1990) Conformational stability of globular proteins. Trends Biochem. Sci. **15**, 14–17
37 Rudolph, R., Siebendritt, R. and Kiefhaber, T. (1992) Reversible unfolding and refolding behavior of a monomeric aldolase from *Staphylococcus aureus*. Protein Sci. **1**, 654–666
38 Ogasahara, K. and Yutani, K. (1997) Equilibrium and kinetic analyses of unfolding and refolding for the conserved proline mutants of tryptophan synthase α-subunit. Biochemistry **36**, 932–940
39 Gualfetti, P. J., Bilsel, O. and Matthews, C. R. (1999) The progressive development of structure and stability during the equilibrium folding of the α-subunit of tryptophan synthase from *Escherichia coli*. Protein Sci. **8**, 1623–1635
40 Andreotti, G., Cubellis, M. V., Di Palo, M., Fessas, D., Sannia, G. and Marino, G. (1997) Stability of a thermophilic TIM-barrel enzyme: indole-3-glycerol phosphate synthase from the thermophilic archaeon *Sulfolobus solfataricus*. Biochem. J. **323**, 259–264
41 Borchert, T. V., Abagyan, R., Jaenicke, R. and Wierenga, R. K. (1994) Design, creation, and characterization of a stable, monomeric triosephosphate isomerase. Proc. Natl. Acad. Sci. U.S.A. **91**, 1515–1518
42 Saab-Rincón, G., Juárez, V. R., Osuna, J., Sánchez, F. and Soberón, X. (2001) Different strategies to recover the activity of monomeric triosephosphate isomerase by directed evolution. Protein Eng. **14**, 149–155
43 Waley, S. G. (1973) Refolding of triosephosphate isomerase. Biochem J. **135**, 165–172
44 Zabori, S., Rudolph, R. and Jaenicke, R. (1980) Folding and association of triosephosphate isomerase from rabbit muscle. Z. Naturforsch. **35**, 999–1004
45 Garza-Ramos, G., Tuena de Gómez-Puyou, M., Gómez-Puyou, A. and Gracy, R. W. (1992) Dimerization and reactivation of triosephosphate isomerase in reverse micelles. Eur. J. Biochem. **208**, 389–395
46 Borchert, T. V., Pratt, K., Zeelen, J., Callens, M., Noble, M. E., Opperdoes, F. R., Michels, P. A. and Wierenga, R. K. (1993) Overexpression of trypanosomal triosephosphate isomerase in *Escherichia coli* and characterisation of a dimer-interface mutant. Eur. J. Biochem. **211**, 703–710
47 Fernández-Velasco, D. A., Sepúlveda-Becerra, M., Galina, A., Darszon, A., Tuena de Gómez-Puyou, M. and Gómez-Puyou, A. (1995) Water requirements in monomer folding and dimerization of triosephosphate isomerase in reverse micelles. Intrinsic fluorescence of conformers related to reactivation. Biochemistry **34**, 361–369
48 Albe, K. R., Butler, M. H. and Wright, B. E. (1990) Cellular concentrations of enzymes and their substrates. J. Theor. Biol. **143**, 163–195
49 Hornby, J. A. T., Luo, J.-K., Stevens, J. M., Wallace, L. A., Kaplan, W., Armstrong, R. N. and Dirr, H. W. (2000) Equilibrium folding of dimeric class μ glutathione transferases involves a stable monomeric intermediate. Biochemistry **39**, 12336–12344
50 Apiyo, D., Jones, K., Guidry, J. and Wittung-Stafshede, P. (2001) Equilibrium unfolding of dimeric desulfoferrodoxin involves a monomeric intermediate: iron cofactors dissociate after polypeptide unfolding. Biochemistry **40**, 4940–4948
51 Bose, K. and Clarck, A. C. (2001) Dimeric procaspase-3 unfolds via a four-state equilibrium process. Biochemistry **40**, 14236–14242
52 Mateu, M. G. (2002) Conformational stability of dimeric and monomeric forms of the C-terminal domain of human immunodeficiency virus-1 capsid protein. J. Mol. Biol. **318**, 519–531

Received 13 September 2002/2 December 2002; accepted 10 December 2002
Published as BJ Immediate Publication 10 December 2002, DOI 10.1042/BJ20021439